

Technical University of Denmark



## Absorption boundary conditions for geometrical acoustics

**Jeong, Cheol-Ho**

*Published in:*  
Internoise 2012

*Publication date:*  
2012

[Link back to DTU Orbit](#)

*Citation (APA):*  
Jeong, C-H. (2012). Absorption boundary conditions for geometrical acoustics. In Interoise 2012

## DTU Library

Technical Information Center of Denmark

---

### General rights

Copyright and moral rights for the publications made accessible in the public portal are retained by the authors and/or other copyright owners and it is a condition of accessing publications that users recognise and abide by the legal requirements associated with these rights.

- Users may download and print one copy of any publication from the public portal for the purpose of private study or research.
- You may not further distribute the material or use it for any profit-making activity or commercial gain
- You may freely distribute the URL identifying the publication in the public portal

If you believe that this document breaches copyright please contact us providing details, and we will remove access to the work immediately and investigate your claim.



## Absorption boundary conditions for geometrical acoustics

Cheol-Ho Jeong<sup>a)</sup>

Acoustic Technology, Department of Electrical Engineering, Technical University of Denmark, DK-2800, Kongens Lyngby, Denmark

**Defining accurate acoustical boundary conditions is of crucial importance for room acoustic simulations. In predicting sound fields using phased geometrical acoustics methods, the absorption coefficients or surface impedances of the boundary surfaces can be used, but no guideline has been developed on which boundary condition produces the best results. In this study, various boundary conditions in terms of normal and random incidence absorption coefficients, and normal incidence surface impedances are used in a phased beam tracing model, and simulated results are validated with boundary element solutions. Two rectangular rooms with uniform and non-uniform absorption distributions are tested. It is concluded that the impedance and random incidence absorption boundary conditions produce reasonable results with some exceptions at low frequencies for acoustically soft materials.**

### 1 INTRODUCTION

The acoustic properties of building elements such as sound absorption coefficients or surface impedances are crucial input data for room acoustic simulations. Absorption coefficients are mainly used for geometrical acoustics methods, whereas wave-based methods generally require surface impedance data. Phase geometrical acoustics methods can adopt both absorption coefficient and surface impedance boundary conditions. This paper mainly aims to evaluate various approximate boundary conditions for a phased beam tracing model. The main question is which boundary condition for the phased geometrical acoustics best approximates locally reacting boundaries. As a validation tool, the boundary element method employing the identical surface impedance boundary condition is used.

Surface impedance boundary conditions are likely to be superior, because they fully describe the physical characteristics of the boundary, i.e., the magnitude and phase changes on reflections. It has been reported that phased geometrical acoustics simulations using surface impedances as boundary conditions agree well with measurements.<sup>1,2</sup> The use of the normal incidence specific surface impedance ( $\zeta_{\text{nor}}$ ) implies that the absorber is of local reaction, because the surface impedance is assumed to be constant over the angle of incidence. If measured

---

<sup>a)</sup> email: chj@elektro.dtu.dk

impedance data are not available, one has to approximately estimate absorption coefficients of the boundary. There are a variety of absorption coefficients to be used in the phased beam tracing: normal incidence and random incidence absorption coefficients ( $\alpha_{nor}$ ,  $\alpha_{rand}$ ), which are assumed to be independent of the incidence angle.  $\alpha_{nor}$  holds only for normal incidence.  $\alpha_{rand}$  strictly assumes random incidence of randomly-phased plane waves onto a large panel, which is unlikely in actual sound fields. However, no comparisons have been conducted among various absorption and impedance boundary conditions. The goal of this study is to find out the boundary condition that best approximates a locally reacting boundary in rectangular rooms and how the simulation error changes with various boundary conditions for the phased beam tracing model.

## 2 ACOUSTIC QUANTITIES AND THEIR RELATIONS

### 2.1 Normal incidence specific surface impedance

This quantity is normally measured by the tube method, by which the impedance at a certain surface is calculated for normal incidence of plane waves. The specific surface impedance is normalized by the characteristic impedance of air by Eq. (1), and will be simply called as the impedance in what follows.

$$\zeta_{nor} = \frac{Z_{nor}}{\rho c}. \quad (1)$$

### 2.2. Normal incidence absorption coefficient

The normal incidence absorption coefficient is also measured by the tube method in the following relationship to the impedance:

$$\alpha_{nor} = 1 - \left| \frac{\zeta_{nor} - 1}{\zeta_{nor} + 1} \right|^2. \quad (2)$$

### 2.3. Random incidence absorption coefficient

The theoretical random incidence absorption coefficient for plane wave incidence on an infinitely large surface can be calculated as follows:<sup>3</sup>

$$\alpha_{rand} = \int_0^{\pi} \alpha_{inf}(\theta_i) \sin(2\theta_i) d\theta_i, \quad (3)$$

where  $\alpha_{inf}(\theta_i)$  is the oblique incidence absorption coefficient at an incidence angle  $\theta_i$  as follows:

$$\alpha_{inf}(\theta_i) = \frac{4 \operatorname{Re}(\zeta_{nor}) \cos \theta_i}{(|\zeta_{nor}| \cos \theta_i)^2 + 2 \operatorname{Re}(\zeta_{nor}) \cos \theta_i + 1}. \quad (4)$$

## 3 METHODS

### 3.1. Test rooms and boundary conditions

Narrow band spectra at 2 Hz intervals were calculated for two rooms that are different in shape and volume: a well proportionate room with dimensions of 1.9×1.4×1 m and a disproportionated room of dimensions of 5×1×1 m. The first room is optimum for achieving evenly spaced modes.<sup>4</sup> For the proportionate room, one source and 54 receivers were chosen. The source position was (0.1, 0.1, 0.4) representing a teacher, because this room was regarded as a ¼ scale model of a lecture room. A total of 54 receivers were positioned with  $x$  changing from 0.15 to 1.75 with steps of 0.2, and  $y$  changing from 0.2 to 1.2 with steps of 0.2, and a fixed  $z$  of 0.3. For the disproportionated room, one source and 36 receivers were positioned. The source was located at (0.1, 0.1, 0.4) and 36 receivers were positioned with  $x$  changing from 0.5 to 4.5 with steps of 0.5, and  $y$  changing from 0.2 to 0.8 with steps of 0.2, and a fixed  $z$  of 0.3.

Various uniform distributions of absorption in the test rooms were examined. A set of impedance data of [40, 20, 10, 7, 4], with acronyms of BC1-BC5, was tested as shown in Table 1, where the corresponding absorption coefficients are also shown, ranging from 0.1 to 0.8. A realistic non-uniform distribution in the proportionate room was also tested. The ceiling, floor, and the side walls were assigned with the impedance data of [5.9, 18, 38], which corresponded to the random incidence absorption coefficients of 0.66, 0.32, and 0.17, respectively.

### 3.2. Reflection modeling in phased beam tracing method

Although the details of PBTM are not explained in this article, the reflection modeling used in the study should be explained. Whichever boundary condition is given, the portion of reflected energy is estimated. From the impedance, the plane wave reflection coefficient is calculated as follows:

$$r(\theta_i) = \frac{\zeta_{nor} \cos(\theta_i) - 1}{\zeta_{nor} \cos(\theta_i) + 1}. \quad (5)$$

Therefore the reflection coefficient is a function of the incidence angle, although the impedance is not angle-dependent. Note that this coefficient is strictly correct for large panels. For grazing incidence or relatively small sized panels, another reflection modeling can be used.<sup>5,6</sup>

For given approximate absorption coefficients, the angle dependence and phase shift on reflection are neglected. Therefore a real-valued and positive reflection coefficient is calculated as

$$r_i = \sqrt{1 - \alpha_i}, \quad (6)$$

where the subscript  $i$  can be “nor”, “rand”, or “field”.

### 3.3. Boundary element models

The boundary element method can solve acoustic problems numerically based on the discretized Helmholtz - Kirchhoff integral equation on a surface mesh.<sup>7</sup> An in-house boundary element model is used for comparisons. For the proportionate, the boundary element model contains 6880 triangular elements with 3442 nodes, of which the  $6\lambda$  per element condition is satisfied up to 1000 Hz. For the disproportionate room, it has 7228 elements and 3616 nodes, therefore its upper cutoff frequency is about 700 Hz. For the two rooms, the linear shape function and seven Gaussian points were used. The boundary element simulations are regarded as the reference simulations.

### 3.4. Error measures

Once transfer functions at 2 Hz intervals are calculated using PBTM and BEM, they are converted to the dB scale re. 1 Pa,  $SPL_{PBTM}$  and  $SPL_{BEM}$ , respectively. In addition, 1/3 octave band spectra are computed based on the narrow band transfer functions, and named as  $SPL_{PBTM,oct}$  and  $SPL_{BEM,oct}$ . Two errors are defined to compare phased beam tracing simulations with boundary element simulations: a narrow band error as  $e_1$  by Eq. (7), and a 1/3 octave band error as  $e_2$  by Eq. (8).

$$e_1(f_c) = \frac{1}{N_{line}} \sum_{i=f_{low}}^{f_{up}} |SPL_{PBTM}(i) - SPL_{BEM}(i)| \text{ (dB)}, \quad (7)$$

$$e_2(f_c) = |SPL_{PBTM,oct}(f_c) - SPL_{BEM,oct}(f_c)| \text{ (dB)}, \quad (8)$$

where  $f_{up}$  and  $f_{low}$  are the upper and lower frequency limit of a frequency band,  $f_c$  is the center frequency of the band, and  $N_{line}$  is the number of frequency lines in the frequency band of

interest. The upper valid frequencies of the proportionate and disproportionate room boundary element models are 1000 Hz and 700 Hz, respectively, therefore the highest center frequencies of the 1/3 octave band are 800 Hz for the proportionate room, and 500 Hz for the disproportionate room. For single-value errors, these errors are averaged over the entire frequency range and over the receiver locations as shown in Tables 1-2.

## 4 RESULTS AND DISCUSSIONS

### 4.1. Uniform absorption in the proportionate room

Average simulation errors in the proportionate room are shown in Table a and Fig. 1. In Table 1, the errors averaged over the frequency bands and receivers are listed. Figure 1 shows the averaged errors over the receiver positions as a function of the frequency for  $\alpha_{\text{nor}}$ ,  $\alpha_{\text{rand}}$ , and  $\zeta_{\text{nor}}$ . For the lowest absorption case, BC1, the 1/3 octave band error is significantly lower than the narrow band error. For  $e_1$ , the random incidence absorption boundary condition shows best results below 200 Hz, whereas the impedance boundary condition yields the best results at higher frequencies. The errors are increased as the frequency increases. For  $e_2$ , the random incidence absorption and impedance boundary conditions yields similar results at frequencies higher than 300 Hz, whereas better agreements are found for the random incidence absorption boundary condition below 300 Hz. The normal incidence absorption coefficient boundary condition yields the worst results.

BC2 shows similar results to BC1. However, the errors become lower than those for BC1, because the simulation errors at the non-resonance frequencies become alleviated for higher absorption cases.<sup>8</sup> Among the three boundary conditions tested, the lowest  $e_1$  is found for the impedance boundary condition, whereas the lowest  $e_2$  is observed using the random incidence absorption. This is mainly ascribed to the fact that the impedance boundary condition slightly underestimates the room response at frequencies below 300 Hz. Beyond the Schroeder frequency of 423 Hz, the simulation accuracy employing the impedance boundary is enhanced and at least comparable to the random incidence absorption boundary condition.

For BC3, the lowest  $e_2$  is found among the tested boundary conditions in Table 1. The impedance boundary condition underestimates the room response at frequencies below 300 Hz, but the errors are reduced above the Schroeder frequency. The best boundary condition in terms of  $e_1$  is the impedance data, whereas a slightly better result is found for the random incidence absorption boundary in terms of  $e_2$ . At frequencies lower than 60 Hz, the normal incidence absorption boundary produces the best results.

For BC4, increased errors are noticed for the random incidence absorption and impedance boundary conditions at low frequencies, whereas the normal incidence absorption boundary condition yields the best result. Above 80 Hz, the errors using the random incidence absorption and impedance boundary conditions tend to be lower than those using the normal incidence absorption coefficient and the best correspondence is found for the impedance boundary condition above the Schroeder frequency.

For BC5, noticeably amplified errors are found at low frequencies, whereas the high frequency errors are quite reduced for the impedance and random incidence boundary condition. The normal incidence absorption coefficient boundary condition yields the lowest error at low frequencies. Above 90 Hz, the errors using the random incidence absorption and impedance boundary conditions become lower, and the best correspondences are found for the impedance boundary condition above the Schroeder frequency. Note that  $e_2$  is larger than  $e_1$  for the impedance boundary condition, because large errors are found at low frequencies.

For the three low absorption cases (BC1-BC3), the random incidence absorption boundary condition best approximates the local reaction boundary condition at low frequencies. Above the Schroeder frequency, the impedance boundary condition agrees best with the boundary element simulations.  $e_2$  is smaller than  $e_1$ , as can be seen in Table 1, which indicates that the errors at the resonance frequencies are likely to be lower than those at the non-resonance frequencies, as also pointed out in Refs. 2,8. PBTM is inherently more accurate at the resonance frequencies, therefore the calculated 1/3 octave band spectra are more accurate. Generally the normal incidence absorption coefficient leads to the most inaccurate simulations, whereas the random/field incidence absorption and impedance boundary condition represent the locally reacting surfaces better. However, for the first few axial modes below 100 Hz, the normal incidence absorption boundary condition yields a similar agreement to the other boundary conditions, which is not surprising, because it is obvious that the sound propagation is one-dimensional. Roughly speaking, below the Schroeder frequency the random incidence absorption boundary condition is better, whereas the accurate results are guaranteed with the impedance boundary condition above the Schroeder frequency. The discrepancies between the random incidence absorption and impedance boundary condition, however, are quite small above the Schroeder frequency.

For the high absorption cases (BC4-BC5), the random incidence absorption and impedance boundary conditions yield very reliable results at high frequencies, whereas the normal incidence absorption produces the best results below 100 Hz. This is related to the sphericity error for high absorptions at very low frequencies, as Lam and Ingard already pointed out,<sup>2,9</sup> because only the plane-wave reflection coefficient is employed in the PBTM simulations. As Ingard found, the sphericity error is indeed related to the angle of incidence: The sphericity error for oblique angle incidence becomes most significant for the lowest impedance, BC5, which supports the predominance of the incident energy at near normal directions.<sup>9</sup> This is the reason why the use of the normal incidence absorption coefficient ensures accurate results in this frequency range below 100 Hz. The best PBTM simulation can be obtained by combining the boundary conditions: the normal incidence absorption coefficient below 70 Hz, the random incidence absorption between 70 to 150 Hz, and the impedance beyond 150 Hz. Because many room acoustic simulations do not require responses in the very low frequency range, say below 100 Hz, the random incidence absorption and impedance boundary conditions are recommended in most cases.

#### **4.2. Non-uniform absorption in the proportionate room**

A non-uniform distribution of absorption was simulated. A typical lecture room has a large amount of absorption on the ceiling, but acoustically reflective walls. The average absorption coefficients in terms of the normal and random incidence absorption were calculated as 0.21 and 0.31, which is similar to BC2 in Table 1. Figure 2 shows the error as a function of the center frequency of the 1/3 octave bands. Similar error trends are found: the impedance boundary condition yields the lowest  $e_1$  except for the very low frequency bands, whereas the random incidence absorption coefficient boundary condition guarantees the lowest  $e_2$  except for the 800 Hz band.

#### **4.3. Uniform absorption in the disproportionate room**

Again the five boundary conditions are assigned on the boundary walls in the disproportionate room. It has been found that the more disproportionate the room, the larger the errors.<sup>8</sup> In Table 2, average errors over the frequency range and the receiver positions are listed. In terms of the narrow band error  $e_1$ , the impedance boundary condition yields the best results.

However, the errors are quite increased compared with the proportional room case, e.g., for BC5, the lowest  $e_1$  and  $e_2$  are increased by 1.2 dB and 2.5 dB, respectively. It turns out that the random incidence absorption boundary condition consistently yields the best results in terms of  $e_2$ , but the differences in  $e_2$  between the random incidence absorption and the impedance boundary condition are less than 0.3 dB as shown in Table 2.

These errors are plotted as a function of the frequency in Fig. 3. The random incidence absorption boundary condition is superior at frequencies below 200 Hz, whereas the impedance boundary condition agrees best with the boundary element simulations above 200 Hz. Note increased errors in Fig. 4(j) at frequencies lower than 100 Hz due to the spherical error, but the error employing the impedance boundary condition decreases significantly, as the frequency increases. The random incidence absorption boundary condition consistently produces the lowest error even at low frequency for low impedances than the normal incidence absorption coefficients in terms of both  $e_1$  and  $e_2$ .

## 5 CONCLUSIONS

This study investigates absorption and impedance boundary conditions for a phased beam tracing model. PBTM simulations employing normal incidence absorption, random incidence absorption, and impedance boundary conditions are compared with boundary element solutions in two rectangular rooms under the assumption of locally reacting boundaries. A large range of impedance and absorption boundary conditions is tested with uniform and non-uniform absorption configurations. The impedance boundary condition is found to yield the best results at higher frequencies above the Schroeder frequency with a few exceptions, whereas the random incidence absorption coefficient boundary conditions are proved to be a robust and accurate boundary condition, in particular at low frequencies. The normal incidence boundary condition generally produces larger errors, and this type of boundary condition is only acceptable for the first few axial room modes and/or for the boundaries having low impedance or high absorption. A non-uniform boundary configuration shows similar error trends for the tested boundary condition. For the disproportionate room, the errors are increased, but the error trends of the boundary conditions investigated are similar to the proportionate room case. By using the plane wave reflection coefficients computed from the impedance boundary condition, the simulation errors can be amplified at frequencies below 100 Hz for low impedance/high absorption. This sphericity error, however, occurs only at very low frequencies, therefore in many cases the impedance boundary condition with plane-wave reflection modeling is a reliable boundary condition.

## 6 REFERENCES

1. J. S. Suh and P. A. Nelson, "Measurement of transient response of rooms and comparison with geometrical acoustic models", *J. Acoust. Soc. Am.*, **105**, 2304-2317, (1999).
2. Y. W. Lam, "Issues for computer modelling of room acoustics in non-concert hall settings", *Acoust. Sci. Tech.*, **26**, 145-155, (2005).
3. H. Kuttruff, *Room Acoustics*, 4th ed., Spon Press, London, (2000).
4. M. M. Loudon, "Dimension ratios of rectangular rooms with good distribution of eigentones", *Acustica*, **24**, 101-104, (1971).

5. C.-H. Jeong, J.-G. Ih, and J. H. Rindel, "An approximate treatment of reflection coefficient in the phased beam tracing method for the simulation of enclosed sound fields at medium frequencies", *Appl. Acoust.*, **69**, 601-613, (2007).

6. J. H. Rindel, "Modeling the angle-dependent pressure reflection factor", *Appl. Acoust.*, **38**, 223-234, (1993).

7. M. Vorlander, *Auralization: fundamentals of acoustics, modelling, simulation, algorithms and acoustic virtual reality*, Springer-Verlag, Berlin, (2008).

8. C.-H. Jeong, and J.-G. Ih, "Effects of source and receiver locations in predicting room transfer functions by a phased beam tracing method", *J. Acoust. Soc. Am.*, **131**, 3864-3875, (2012).

9. U. Ingard, "On the reflection of a spherical sound wave from an infinite plane", *J. Acoust. Soc. Am.*, **23**, 329-335, (1951).

*Table 1 – Errors for five uniform absorption conditions and one non-uniform condition in the proportionate room. The surface impedance, corresponding normal, random, field incidence coefficients, and Schroeder frequencies are indicated. The lowest errors are indicated in bold.*

	$\zeta_{nor}$	$\alpha_{nor}$	$\alpha_{rand}$	$f_{Sch}$	Mean $e_1$			Mean $e_2$		
					$\alpha_{nor}$	$\alpha_{rand}$	$\zeta_{nor}$	$\alpha_{nor}$	$\alpha_{rand}$	$\zeta_{nor}$
BC1	40	0.10	0.17	566	4.0	2.2	<b>1.8</b>	2.2	<b>0.6</b>	0.9
BC2	20	0.18	0.30	423	3.7	1.4	<b>1.2</b>	2.4	<b>0.6</b>	0.9
BC3	10	0.33	0.49	331	3.7	1.2	<b>1.0</b>	2.5	<b>0.9</b>	1.0
BC4	7	0.43	0.60	299	3.7	1.4	<b>1.0</b>	2.6	<b>1.1</b>	<b>1.1</b>
BC5	4	0.64	0.79	260	3.5	1.8	<b>1.2</b>	2.6	<b>1.7</b>	<b>1.7</b>
Non-uniform		0.21	0.31	414	3.5	2.5	<b>2.2</b>	2.9	<b>1.2</b>	1.5

*Table 2 – Errors for five uniform absorption conditions and one non-uniform condition in the disproportionate room. The surface impedance and Schroeder frequencies are indicated. The lowest errors are indicated in bold.*

	$\zeta_{nor}$	$f_{Sch}$	Mean $e_1$			Mean $e_2$		
			$\alpha_{nor}$	$\alpha_{rand}$	$\zeta_{nor}$	$\alpha_{nor}$	$\alpha_{rand}$	$\zeta_{nor}$
BC1	40	416	4.0	2.0	<b>1.6</b>	3.1	<b>1.2</b>	1.4
BC2	20	311	4.5	2.0	<b>1.5</b>	3.9	<b>1.4</b>	1.7
BC3	10	243	5.4	2.8	<b>1.7</b>	4.4	<b>2.0</b>	2.2
BC4	7	219	6.1	3.5	<b>1.9</b>	4.9	<b>2.5</b>	2.8
BC5	4	192	7.3	5.3	<b>2.4</b>	6.2	<b>4.1</b>	4.2



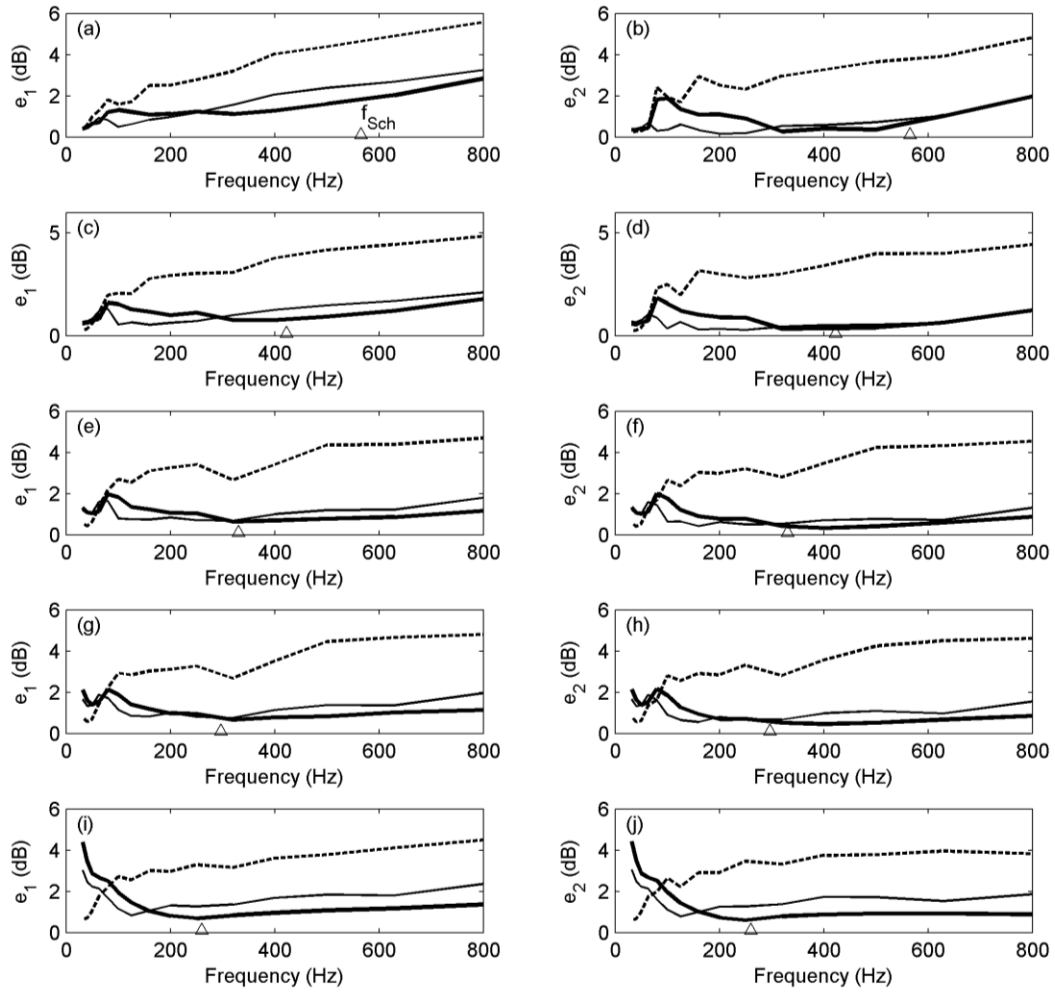


Fig. 1 – Errors in the proportionate room. (a),(c),(e),(g),(i)  $e_1$ ; (b),(d),(f),(h),(j)  $e_2$ . (a),(b) BC1; (c),(d) BC2; (e),(f) BC3; (g),(h) BC4; (i),(j) BC5. — —,  $\alpha_{nor}$ ; —,  $\alpha_{rand}$ ; — —,  $\zeta_{nor}$ .

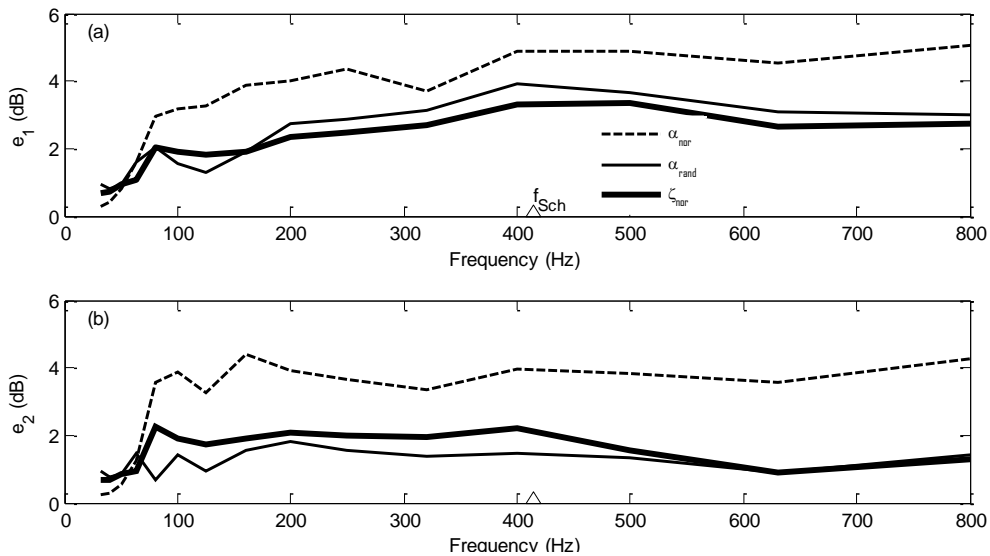


Fig. 2 – Errors in the proportionate room for the non-uniform distribution. (a)  $e_1$ ; (b)  $e_2$ .

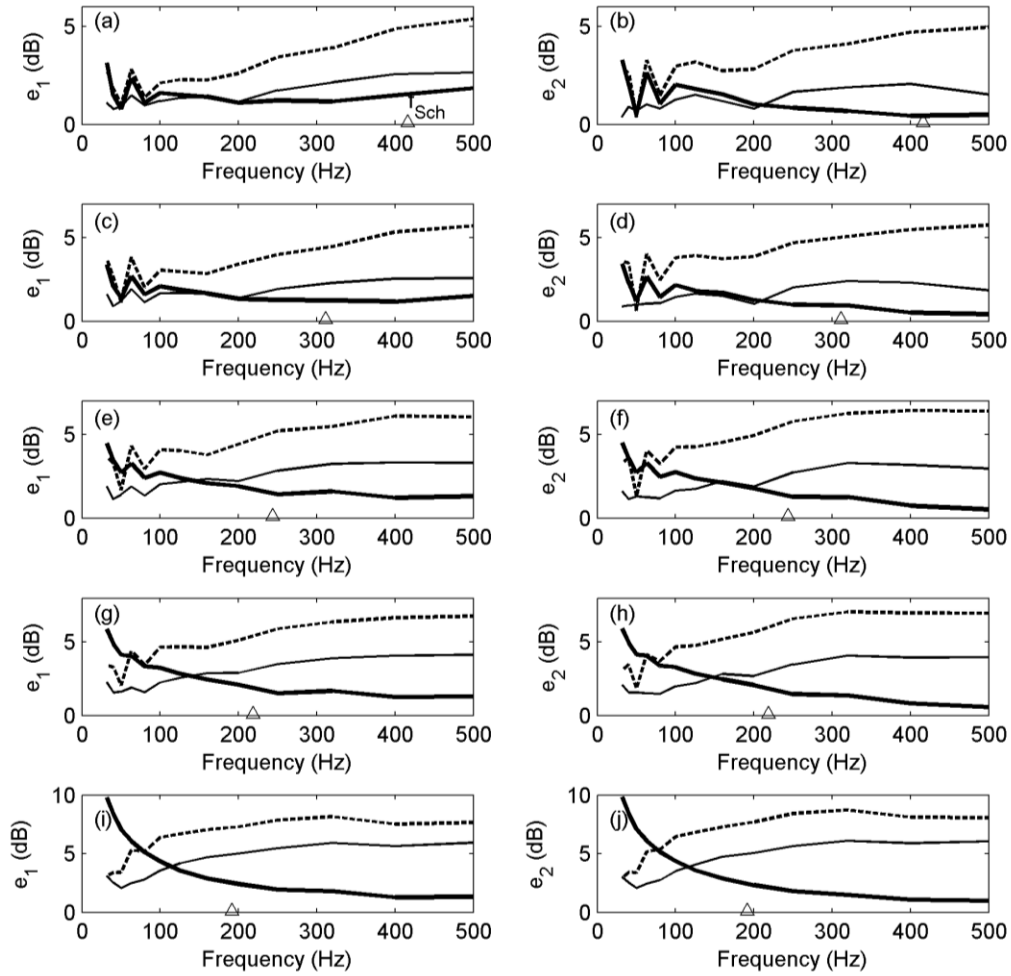


Fig. 3— Errors in the disproportionate room. (a),(c),(e),(g),(i)  $e_1$ ; (b),(d),(f),(h),(j)  $e_2$ . (a),(b) BC1; (c),(d) BC2; (e),(f) BC3; (g),(h) BC4; (i),(j) BC5. — —,  $\alpha_{nor}$ ; —,  $\alpha_{rand}$ ; —,  $\zeta_{nor}$ .  $\Delta$  indicates the Schroeder frequency.